Journal of Manufacturing Processes 13 (2011) 24–29

Contents lists available at ScienceDirect

Journal of Manufacturing Processes

journal homepage: www.elsevier.com/locate/manpro

Technical paper

A tuned holder for increased boring bar dynamic stiffness

Lonnie Houck III [a], Tony L. Schmitz [a,*], K. Scott Smith [b]

[a] Department of Mechanical and Aerospace Engineering, University of Florida, Gainesville, FL 32611, USA

[b] Mechanical Engineering and Engineering Science Department, University of North Carolina at Charlotte, Charlotte, NC 28223, USA

ARTICLE INFO

Article history:
Received 31 May 2010
Received in revised form
9 September 2010
Accepted 21 September 2010
Available online 14 October 2010

ABSTRACT

In this paper, the design and testing of a tuned holder that increases the dynamic stiffness of boring bars is described. By matching the holder natural frequency to the clamped–free boring bar natural frequency, a new dynamic system is obtained with decreased vibration magnitude and reduced susceptibility to chatter. In this approach, the flexible holder supports the boring bar and effectively acts as a dynamic absorber for the clamped boring bar. Design trends are explored using an analytical receptance coupling model and experimental validation is provided.

1. Introduction

During machining operations, vibratory motion between the tool and workpiece can lead to reduced performance. In particular, self-excited vibration, or chatter, causes poor surface finish, tool damage, and other unwanted effects. When chatter does occur, the machining parameters must be modified, and productivity may be reduced (e.g., the material removal rate may be limited by the maximum allowable depth of cut to avoid chatter). One example of tools that may encounter excessive vibration is boring bars, which are used to produce internal cylindrical and conical surfaces. A primary difficulty in their use is that, because they enlarge holes that tend to be deep and narrow, they are often long and have small diameters. This naturally leads to low stiffness. Therefore, a variable cutting force during boring operations causes the tool to deflect and leave behind a wavy surface. When the cutting edge encounters this wavy surface in the next revolution, the relative phasing can lead to increased force and deflection through regenerative chatter.

For both single-point and multi-point machining processes in general, it is well known that the allowable chatter-free chip width depends on the cutting system's frequency response function (as reflected at the tool point) and the selected cutting conditions. Early work by Hahn, Tobias, Tlusty, and Merritt [1–7] led to the development of graphical depictions of the boundary between stable and unstable machining conditions, which are referred to as stability lobe diagrams. In these plots, spindle speed is typically selected as the independent variable and chip width as the dependent variable. Stability lobe diagrams identify increased chatter-free chip widths for spindle speeds (or tooth passing frequencies in multi-point operations) that are equal to integer fractions of the cutting system's natural frequency which corresponds to the most flexible vibration mode. While these spindle speeds can lead to substantial increases in chip width in many milling applications, the improvement in most boring/turning applications is small. Therefore, other passive and active techniques have been developed to improve chatter resistance. Rivin provides a comprehensive overview of these and other issues related to the dynamic stiffness (the product of stiffness and damping) of tools and holders [8]. He categorizes these techniques as:

- reduction of cutting forces
- high damping clamping devices
- bars with anisotropic stiffness
- periodic variation of cutting conditions
- enhancement of structural stiffness
- passive vibration absorbers
- active dampers
- active correction systems.

Selected examples of these approaches include commercially available boring bars with internal passive vibration absorbers, active vibration control [9–12], bar material selection for increased dynamic stiffness [13–15], actuation of an internal electrorheological fluid [16], error compensation [17], and holder modification [18].

Here, a new method to reduce tool vibrations by providing a flexible holder with dynamics tuned to the boring bar dynamics is described. The flexible holder supports the boring bar and acts as a dynamic absorber (for the boring bar). The flexible holder natural frequency is approximately matched to the clamped–free natural frequency of the bar and reduces the magnitude of vibration at

* Corresponding author. Tel.: +1 352 392 8909; fax: +1 352 392 1071.
E-mail addresses: lhouck23@ufl.edu (L. Houck III), tschmitz@ufl.edu (T.L. Schmitz), kssmith@uncc.edu (K. Scott Smith).

1526-6125/$ – see front matter
doi:10.1016/j.jmapro.2010.09.002

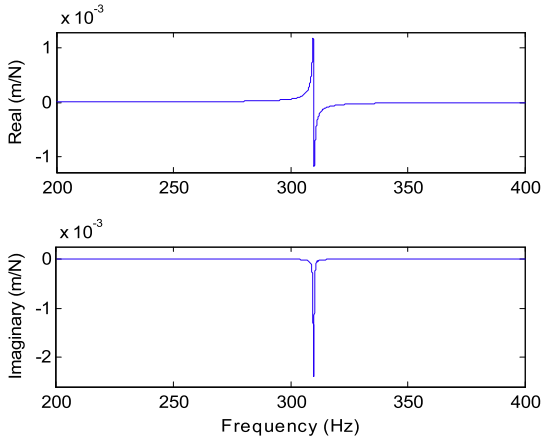

Fig. 1. Clamped–free response of a 12:1 boring bar.

the bar–holder assembly's free (cutting) end. The advantage of this approach is that standard boring bars can be used and the monolithic holder design is straightforward to manufacture. An analytical solution which applies Euler–Bernoulli beam theory and receptance coupling to explore trends is first presented and then the final holder design is detailed. Frequency response (receptance) measurements of a prototype boring bar–holder assembly are provided and compared to the clamped–free response of the boring bar alone. Increased dynamic stiffness is demonstrated for the boring bar–holder assembly. Although not expressly demonstrated here, prior turning stability research has shown that increased dynamic stiffness tends to subsequently increase the (asymptotic) stability limit for boring operations [4–7].

2. Receptance coupling model

Closed-form, Euler–Bernoulli beam receptances [19] were used to describe an ISO A10-SCLPR2 NE4 boring bar with a 12:1 length to diameter (L: D) ratio. (Note that there is no restriction on the L: D ratio that can be used in this approach.) A diameter, d, of 15.9 mm was chosen because this is on the order of the smallest available diameter for commercial boring bars with internal dynamic absorbers. Fig. 1 shows the analytical frequency response function (FRF) for lateral vibration, x, at the free end (coordinate 1) due to an external force, f, applied at the free end for the clamped–free beam model of the steel boring bar. It was developed using Eq. (1), where $E = 200$ GPa is the elastic modulus, $I = \frac{\pi d^4}{64}$ is the area moment of inertia, and $\eta = 0.0015$ is the unitless solid damping factor. Also, $\lambda^4 = \frac{\omega^2 m}{EI(1+i\eta)L}$, where ω is the frequency (rad/s), m is the beam mass, and L is the length [19].

$$h_{11} = \frac{x_1}{f_1} = \frac{\sin(\lambda L)\cosh(\lambda L) - \cos(\lambda L)\sinh(\lambda L)}{EI\,(1+i\eta)\,\lambda^3\,(\cos(\lambda L)\cosh(\lambda L)+1)}. \tag{1}$$

Using a modal analysis peak picking method [20] on the FRF shown in Fig. 1, a stiffness value of 2.79×10^5 N/m and a viscous damping ratio of 6.5×10^{-4} (0.5η) were determined for the 309.9 Hz boring bar bending mode. A single degree of freedom spring–mass–damper representation of a clamped–free holder was then defined with a stiffness value of $20\cdot(2.79 \times 10^5)$ N/m, but the same natural frequency and damping ratio as the clamped–free boring bar. Next, the holder model was rigidly coupled to a free–free model of the boring bar using the receptance coupling approach [19]. The free–free beam FRFs were defined according to Eqs. (2)–(5), where 1 is the free end coordinate, 2 is the end clamped to the holder, θ_i ($i = 1, 2$) is rotation, and m_i is an external couple.

$$\begin{aligned}
h_{11} &= \frac{x_1}{f_1} = \frac{\sin(\lambda L)\cosh(\lambda L) - \cos(\lambda L)\sinh(\lambda L)}{EI\,(1+i\eta)\,\lambda^3\,(\cos(\lambda L)\cosh(\lambda L)-1)}\\
l_{11} &= \frac{x_1}{m_1} = \frac{\sin(\lambda L)\sinh(\lambda L)}{EI\,(1+i\eta)\,\lambda^2\,(\cos(\lambda L)\cosh(\lambda L)-1)}\\
n_{11} &= \frac{\theta_1}{f_1} = l_{11}\\
p_{11} &= \frac{\theta_1}{m_1} = \frac{\cos(\lambda L)\sinh(\lambda L) + \sin(\lambda L)\cosh(\lambda L)}{EI\,(1+i\eta)\,\lambda\,(\cos(\lambda L)\cosh(\lambda L)-1)}
\end{aligned} \tag{2}$$

$$\begin{aligned}
h_{22} &= \frac{x_2}{f_2} = h_{11}\\
l_{22} &= \frac{x_2}{m_2} = -l_{11}\\
n_{22} &= \frac{\theta_2}{f_2} = l_{22}\\
p_{22} &= \frac{\theta_2}{m_2} = p_{11}
\end{aligned} \tag{3}$$

$$\begin{aligned}
h_{12} &= \frac{x_1}{f_2} = \frac{\sin(\lambda L) - \sinh(\lambda L)}{EI\,(1+i\eta)\,\lambda^3\,(\cos(\lambda L)\cosh(\lambda L)-1)}\\
l_{12} &= \frac{x_1}{m_2} = \frac{\cosh(\lambda L) - \cos(\lambda L)}{EI\,(1+i\eta)\,\lambda^2\,(\cos(\lambda L)\cosh(\lambda L)-1)}\\
n_{12} &= \frac{\theta_1}{f_2} = -l_{12}\\
p_{12} &= \frac{\theta_1}{m_2} = \frac{\sin(\lambda L) + \sinh(\lambda L)}{EI\,(1+i\eta)\,\lambda\,(\cos(\lambda L)\cosh(\lambda L)-1)}
\end{aligned} \tag{4}$$

$$\begin{aligned}
h_{21} &= \frac{x_2}{f_1} = h_{12}\\
l_{21} &= \frac{x_2}{m_1} = n_{12}\\
n_{21} &= \frac{\theta_2}{f_1} = l_{12}\\
p_{21} &= \frac{\theta_2}{m_1} = p_{12}.
\end{aligned} \tag{5}$$

The coupling was completed using Eq. (6) [21,22], where $H_{11} = \frac{X_1}{F_1}$ is the required assembly FRF (at the tool's free end), $R_{ij} = \begin{bmatrix} h_{ij} & l_{ij} \\ n_{ij} & p_{ij} \end{bmatrix}$, and only the $h_{33} = \frac{x_3}{f_3}$ holder FRF was modeled (l_{33}, n_{33}, and p_{33} were assumed rigid). A schematic representation of the model is provided in Fig. 2. The predicted responses for the boring bar–holder assembly and clamped–free boring bar are compared in Fig. 3.

$$\begin{bmatrix} H_{11} & L_{11} \\ N_{11} & P_{11} \end{bmatrix} = R_{11} - R_{12}\,(R_{22} + R_{33})^{-1}\,R_{21}. \tag{6}$$

Fig. 3 shows that the single degree of freedom clamped–free bar FRF (within the selected frequency range) becomes a two degree of freedom response with the addition of the holder. The peak magnitude is reduced from 2.39×10^{-3} m/N (309.9 Hz) to 1.63×10^{-3} m/N (256.1 Hz); this represents a 32% peak reduction or 1.5 times dynamic stiffness increase. The increased dynamic stiffness of the assembly is counterintuitive (i.e., adding a flexible element increases the assembly stiffness), but is similar in nature to the well-known dynamic absorber effect. Additionally, because the holder is 20 times stiffer than the boring bar, the subsequent increase in static (zero frequency) compliance is not significant: 3.70×10^{-6} m/N for the clamped–free bar versus 3.88×10^{-6} m/N for the assembly.

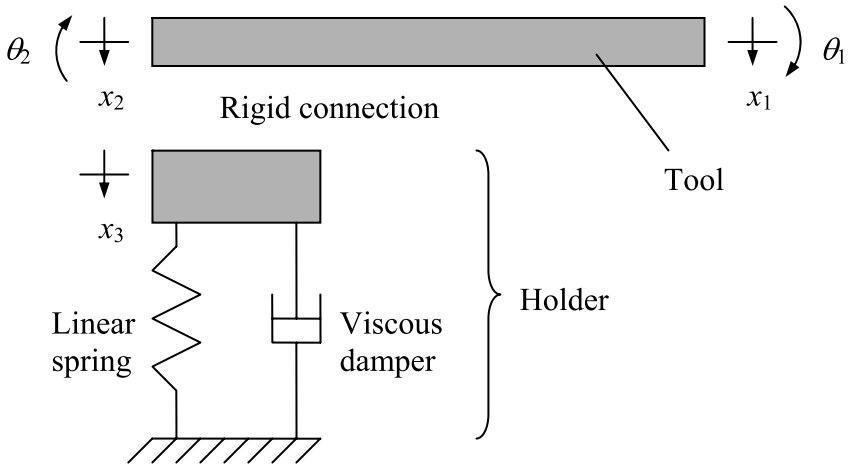

Fig. 2. Schematic representation of receptance coupling model for the boring bar–holder assembly.

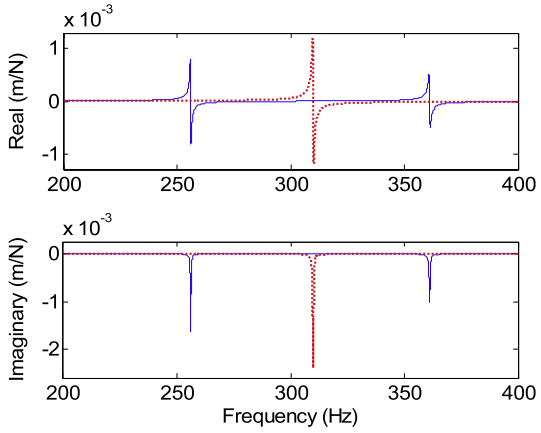

Fig. 3. Boring bar–holder assembly (solid line) and clamped–free boring bar (dotted line) responses.

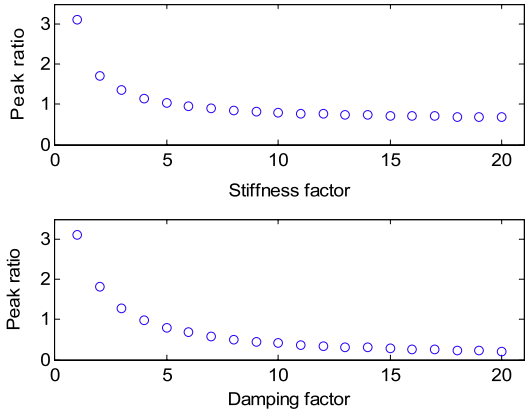

Fig. 4. Peak ratio for stiffness (top) and damping (bottom) factors.

The receptance coupling model was next used to evaluate the individual effects of the holder stiffness and damping on the assembly FRF. Fig. 4 displays: (top panel) the ratio of the boring bar–holder assembly peak magnitude to the clamped–free boring bar peak magnitude (labeled as peak ratio) as a function of a stiffness factor, equal to the holder stiffness divided by the boring bar stiffness; and (bottom panel) an analogous damping factor. In both instances, the bar and holder natural frequencies were matched for all factor values. Additionally, for the stiffness factor analysis the damping factor was 1 and for the damping factor analysis the stiffness factor was 1.

In Fig. 4, a decrease in the peak ratio (i.e., the assembly stiffness increases relative to the clamped–free boring bar alone) is observed for an increase in the stiffness/damping factors. It is seen that the damping effect is stronger and that the decrease is approximately logarithmic in both instances. Also, stiffness/damping factors greater than 5 are required to improve the system dynamic stiffness. Interestingly, the reduced peak ratio trend continues to hold even for large stiffness factors. For example, if the holder is 1×10^4 times stiffer than the clamped–free bar, interaction still occurs. Fig. 5 shows this result. Naturally, for very large stiffness factors (order of 1×10^7) the assembly response begins to resemble the original clamped–free response and the peak ratio approaches 1.

Finally, the influence of the holder's natural frequency relative to the boring bar's clamped natural frequency was investigated. A stiffness factor of 20 was selected, while the damping factor was set to 1. Using the receptance coupling model, the ratio of the holder natural frequency to the clamped–free bar natural frequency, or frequency factor, was varied between 0.75 and 1.25 (±25% variation from the matched condition). Fig. 6 displays the ratio of the boring bar–holder assembly peak magnitude to the clamped–free boring bar peak magnitude as a function of the frequency factor. First, it is seen that the matched condition does not yield the maximum dynamic stiffness increase. For the 12:1 boring bar/stiffness factor combination considered here, the best frequency factor is 0.925 (i.e., the holder's natural frequency is 92.5% of the clamped–free boring bar's natural frequency). This case is shown in Fig. 7. Second, the assembly's dynamic stiffness exhibits sensitivity to the frequency factor. For example, a 10% increase in the frequency factor from 1 to 1.1 in Fig. 6 leads to a peak ratio increase of 20% (0.68 to 0.82).

3. Prototype design

The primary design considerations revealed by the receptance coupling analysis were that: (1) the holder natural frequency should be approximately matched to the clamped–free boring bar natural frequency and the assembly dynamic stiffness is sensitive to their ratio; and (2) the holder stiffness and damping should be significantly higher than the corresponding values for the clamped–free boring bar alone. These considerations must naturally be balanced by the existing design constraints. First, it is challenging to add damping to structures without increasing their

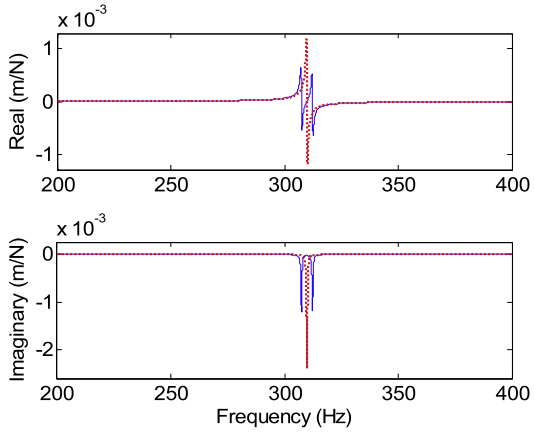

Fig. 5. Boring bar–holder (solid line) and clamped–free bar (dotted line) responses for a stiffness factor of 1×10^4.

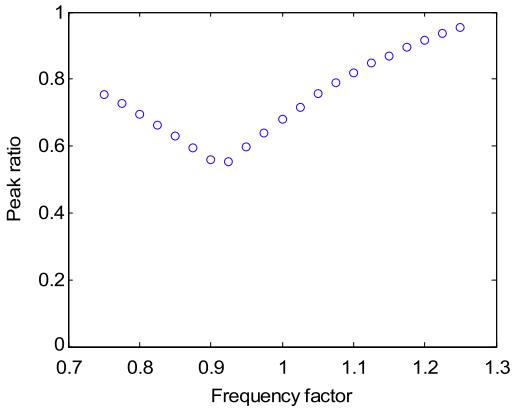

Fig. 6. Peak ratio for variable holder natural frequency.

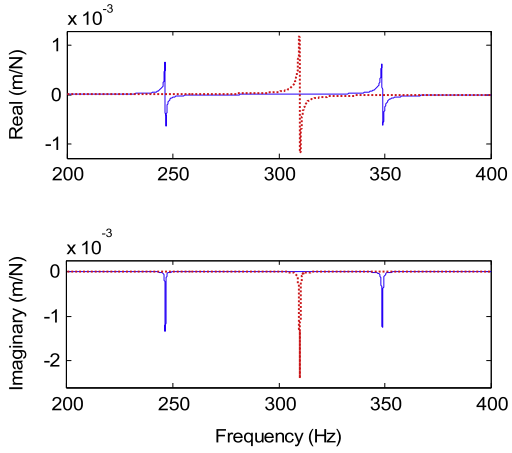

Fig. 7. Boring bar–holder assembly (solid line) and clamped–free boring bar (dotted line) responses for 0.925 frequency factor from Fig. 6.

mechanical complexity; an example previously used in machining applications is shear layer damping [23]. Second, the boring bar natural frequency depends strongly on its length and the holder connection. For these reasons, the focus of the holder design was high stiffness combined with convenient tuning of its natural frequency without requiring adjustments to the boring bar.

The design concept is shown in Fig. 8. It includes: (1) a 50.8 mm diameter monolithic aluminum holder (Fig. 9) with circular notches to set the natural frequency/stiffness and a dovetail base connection; (2) a brass sleeve to enable "mass tuning",

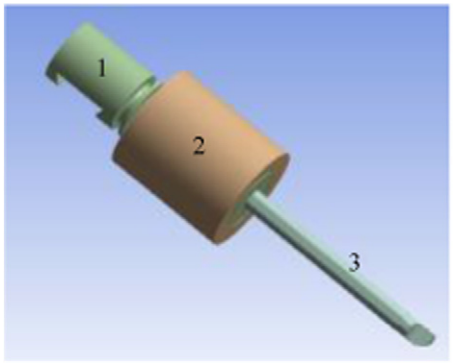

Fig. 8. Boring bar–holder assembly design concept (1 — holder, 2 — sleeve, and 3 — boring bar).

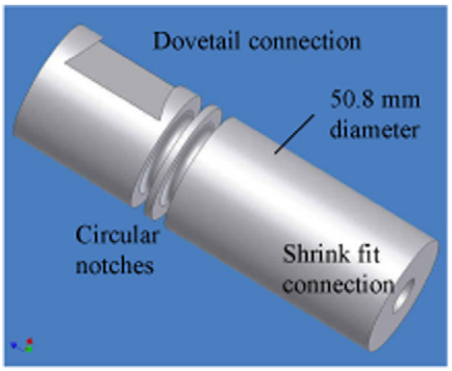

Fig. 9. Notched flexure holder with dovetail base and thermal shrink fit boring bar connections.

in which the natural frequency of the holder is adjusted by modifying the sleeve's axial position and, therefore, the holder–sleeve assembly's modal mass; and (3) the steel boring bar, which is inserted in the holder using a thermal shrink fit connection (this is enabled by the higher thermal expansion of the aluminum holder relative to the steel boring baring). The mass tuning approach using the sleeve's axial position provides a preferred alternative to adjusting the boring bar's overhang length in order to tune the assembly dynamics (as shown in Fig. 6, for example). The reader may note that this design is inherently axisymmetric so that improved dynamic stiffness with nominally the same response in all radial directions can be achieved.

4. Results and discussion

The following set-ups were used for FRF measurements: (1) the boring bar was clamped in a vise with a 12:1 L:D ratio to simulate clamped–free boundary conditions; (2) the boring bar was inserted in the holder–sleeve (again using the 12:1 L:D) and the entire assembly was clamped in the vise (see Fig. 10); (3) the holder–sleeve–boring bar assembly was mounted to a standard dovetail holder; and (4) the sleeve axial position was varied in the dovetail set-up to see the effect. The FRF measurements were completed by exciting the free end of the boring bar with a modal hammer and recording the response using a low mass accelerometer.

A comparison of the measurements for the two vise set-ups is provided in Fig. 11. As shown by the receptance coupling model, the dynamic stiffness for the assembly is higher than for the clamped–free boring bar alone. The peak response is reduced from

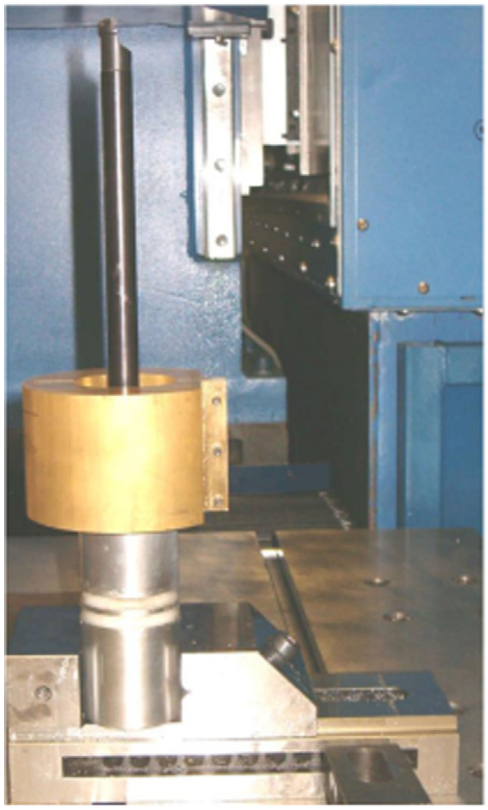

Fig. 10. Set-up for frequency response measurements of the vise–holder–sleeve–boring bar assembly.

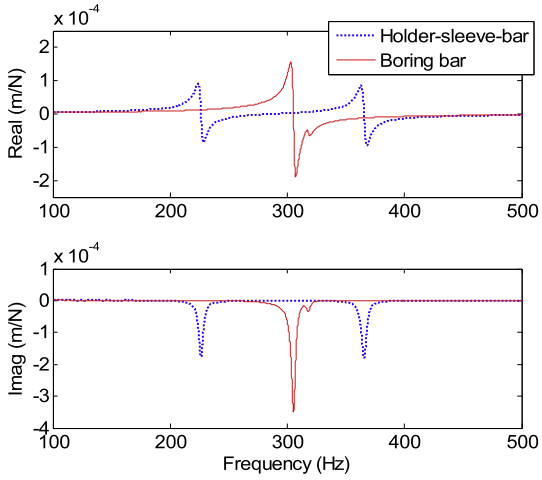

Fig. 11. Measurement results for the vise set-up: boring bar alone and holder–sleeve–boring bar assembly.

3.49×10^{-4} m/N (305 Hz) to 1.80×10^{-4} m/N (365.5 Hz); this represents a 48% peak magnitude reduction or 1.9 times dynamic stiffness increase.

The measurement result for the dovetail set-up is displayed in Fig. 12. Similar behavior is observed as in Fig. 11. The peak response is reduced from 3.49×10^{-4} m/N (305 Hz) to 1.09×10^{-4} m/N (365.5 Hz); this represents a 69% peak magnitude reduction. However, additional modes are also seen, and the entire response is shifted to the left (lower frequencies). This behavior makes sense given the non-rigid coupling present in the dovetail connection. The increased dynamic stiffness relative to the vise

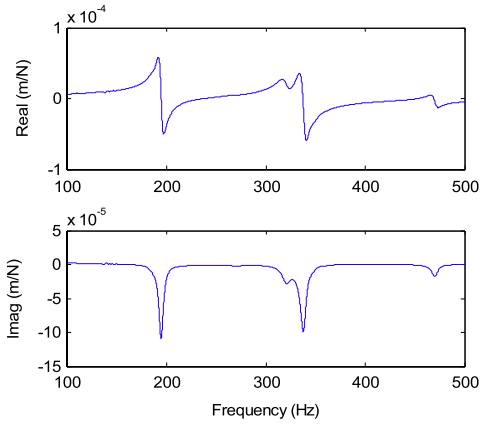

Fig. 12. Measurement results for the dovetail set-up of the holder–sleeve–boring bar assembly.

set-up is presumably due to increased damping in the non-rigid dovetail interface.

Finally, the sleeve position was axially varied for the dovetail set-up to demonstrate the resulting influence on the assembly FRF. Measurement results (real part of FRF) are provided in Fig. 13, where the progression is for sleeve positions from the holder notches (1) toward the free end of the holder (9); the total range was 70 mm. For position 1, the effective modal mass of the sleeve was the lowest and the frequency match between the holder and clamped–free boring bar was poor. Therefore, the dynamic interaction was weak and the assembly response appears to be single degree of freedom (within the selected frequency range). At position 6, minimum assembly magnitude is obtained. As the effective sleeve modal mass is increased, however, the natural frequencies are again mismatched and the peak magnitude grows. These results show that the sleeve tuning approach offers sufficient flexibility to tailor the assembly dynamics to a minimum magnitude for a selected L: D ratio.

5. Conclusions

A tuned holder design was described that provides increased dynamic stiffness for the holder–boring bar assembly. The design geometry is simple and relies simply on an approximate natural frequency match between the holder and clamped–free boring bar. There are no significant restrictions on the holder design or material. Aluminum was selected for this study for fabrication convenience and to enable the thermal shrink fit connection with a commercially available steel boring bar. Additionally, the concept of mass tuning was demonstrated by adding a sleeve to the holder. By varying the axial position of the sleeve, its effective modal mass is changed, and the assembly dynamics were tuned to the minimum magnitude condition. Experimental results were provided and a 69% magnitude reduction was demonstrated for the assembly relative to a clamped–free boring bar (of the same 12:1 length to diameter ratio) alone.

Acknowledgements

This work was supported by the National Science Foundation (DMI-0555645) and Kennametal, Inc. Any opinions, findings, and conclusions or recommendations expressed in this material are those of the authors and do not necessarily reflect the views of these agencies.

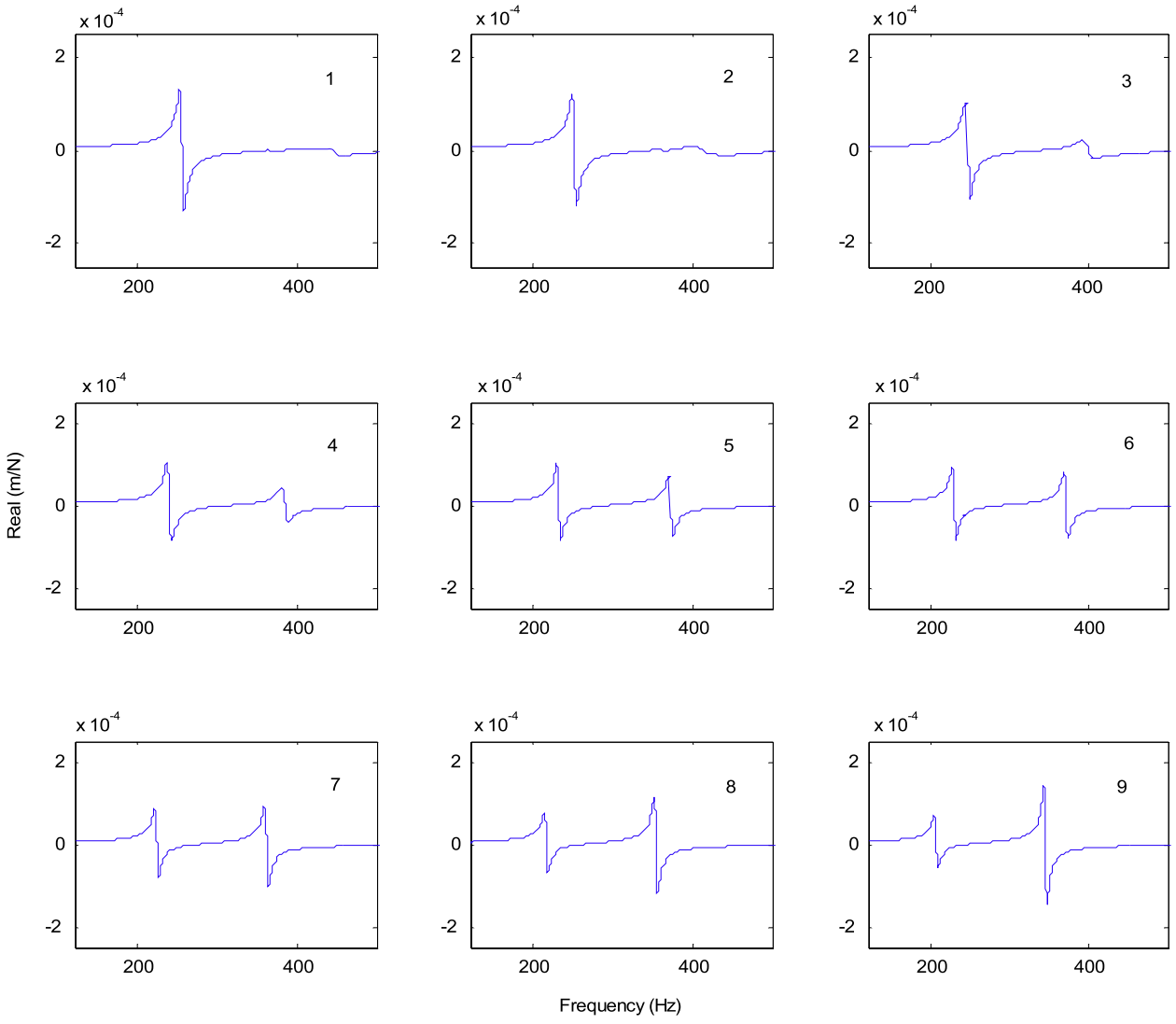

Fig. 13. Effect of varying the sleeve's axial position on the assembly FRF. The sleeve is located at the holder notches for position 1 and displaced 70 mm toward the free end of the holder for position 9.

References

[1] Hahn RS. Design of Lanchester damper for elimination of metal-cutting chatter. Transactions of the ASME 1951;73:331–5.
[2] Hahn RS. Metal-cutting chatter and its elimination. Transactions of the ASME 1953;75:1073–80.
[3] Gurney JP, Tobias SA. A graphical analysis of regenerative machine tool instability. ASME Journal of Engineering for Industry 1962;84:103–12.
[4] Tlusty J, Polacek M. The stability of the machine-tool against self-excited vibration in machining. In: Proceedings of the conference on international research in production engineering. 1963. p. 465–74.
[5] Merritt HE. Theory of self-excited machine-tool chatter. ASME Journal of Engineering for Industry 1965;17:447–54.
[6] Tobias SA. Machine tool vibration. Hoboken (NJ): Wiley; 1965.
[7] Hanna NH, Tobias SA. A theory of nonlinear regenerative chatter. ASME Journal of Engineering for Industry 1974;96:247–55.
[8] Rivin E. Tooling structure: interface between cutting edge and machine tool. Annals of the CIRP 2000;49(2):591–634.
[9] Klein RG, Nachtigal CL. The application of active control to improve boring bar performance. Journal of Dynamic Systems, Measurement, and Control 1975; 97:179–83.
[10] Tewani SG, Rouch KE, Walcott BL. A study of cutting process stability of a boring bar with active dynamic absorber. International Journal of Machine Tools and Manufacture 1995;35:91–108.
[11] Browning DR, Golioto I, Thompson NB. Active chatter control system for long-overhang boring bars. In: Proceedings of the SPIE smart structures and materials conference. vol. 3044. 1997. p. 270–80.
[12] Pratt JR, Nayfeh AH. Chatter control and stability analysis of a cantilever boring bar under regenerative cutting conditions. Philosophical Transactions: Mathematical, Physical and Engineering Sciences 2001;359(1781):759–92.
[13] Lee DG, Suh NP. Manufacturing and testing of chatter free boring bars. Annals of the CIRP 1988;37(1):365–8.
[14] Lee DG, Hwang HY, Kim JK. Design and manufacture of a carbon fiber epoxy rotating boring bar. Composite Structures 2003;60:115–24.
[15] Nagano S, Koizumi T, Fujii T, Tsujiuchi N, Ueda H, Steel K. Development of a composite boring bar. Composite Structures 1997;38(1–4):531–9.
[16] Wang M, Fei R. On-line chatter detection and control in boring based on an electrorheological fluid. Mechatronics 2001;11:779–92.
[17] Gao D, Yao YX, Chiu WM, Lam FW. Accuracy enhancement of a small overhung boring bar servo system by real-time error compensation. Precision Engineering 2002;26:456–9.
[18] Takeyama H, Iijima N, Nishiwaki N, Komoto K. Improvement of dynamic rigidity of tool holder by applying high-damping material. Annals of the CIRP 1984;33(1):249–52.
[19] Bishop RED, Johnson DC. The mechanics of vibration. Cambridge: Cambridge University Press; 1960.
[20] Ewins D. Modal testing: theory and practice. Somerset (England): Research Studies Press, Ltd.; 1995.
[21] Schmitz T, Duncan GS. Three-component receptance coupling substructure analysis for tool point dynamics prediction. Journal of Manufacturing Science and Engineering 2005;127(4):781–90.
[22] Schmitz T, Smith KS. Machining dynamics: frequency response to improved productivity. NY: Springer; 2009.
[23] Ziegert J, Sterling R, Stanislaus C, Schmitz T. Enhanced damping in long slender endmills. Transactions of NAMRI/SME 2004;32:1–7.